ULTRA-FAST BROADBAND EMI MEASUREMENT IN TIME DOMAIN USING CLASSICAL SPECTRAL ESTIMATION

Florian Krug, *Student Member, IEEE* and
Peter Russer, *Fellow, IEEE*

Lehrstuhl für Hochfrequenztechnik, Technische Universität München
Arcisstr. 21, D-80333 Munich, Germany, eMail: krug@ei.tum.de

Abstract—**In this paper, a novel ultra-fast, broadband time domain EMI measurement system is described. Measurements were performed in the 30 - 1000 MHz range. The signals from the antenna are digitized and processed by computer in order to obtain Fast-Fourier Transform (FFT) as well as Welch and Bartlett Periodograms. Correction of errors originating from the frequency characteristics of antenna, cable and oscilloscope is made by digital signal processing. With the presented time domain measurement system the measurement time can be reduced by a factor of 10. The results obtained with the described system have been compared with measurements performed with a conventional EMI receiver. Over the whole frequency range from 30 to 1000 MHz the deviations have been below 3 dB.**

I. INTRODUCTION

In the past and currently, radio noise and electromagnetic interference (EMI) are measured and characterized by superheterodyne radio receivers. The disadvantage of this method is the quite long measurement time of typically 30 minutes [1] for a frequency band from 30 to 1000 MHz [2]. Time-domain EMI measurements in the lower frequency range have been published in [1], [3] and [4]. In this paper a novel ultra-fast, time-domain measurement setup including the system for the 30 - 1000 MHz frequency range is described.

II. TIME-DOMAIN EMI MEASUREMENT SYSTEM

The block diagram of the experimental setup consisting of the time-domain measurement system and a conventional EMI receiver is depicted in Fig. 1. The EMI receiver is used for comparison. Table I summarizes the components of the time-domain measurement setup. The time-domain measurement system consists of broad-band antenna, switching unit, EMI receiver, amplifier, low-pass filter, oscilloscope and a personal computer.

The broad-band antenna combines the characteristics of a biconical and a log-periodic antenna to facilitate measurement from 30 to 1000 MHz. The amplifier is required due to the low sensitivity of the oscilloscope. The anti-aliasing filter limits the signal bandwidth according to the requirement of the sampling theorem. The oscilloscope has an analog bandwidth of 1 GHz. The data are transmitted via a GPIB bus to the personal computer. The equipment under test (EUT) is a commercial laptop with a 200 MHz clock frequency. The measurements on the laptop are performed in the power-on mode, supplied from the internal battery. All measurements have been made in an anechoic chamber with 1 m distance between the vertically polarized antenna and the EUT. The measurement scenario is shown in Fig. 2.

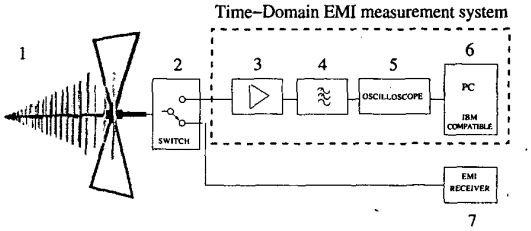

Fig. 1. Time-domain EMI measurement system block diagram

TABLE I
TIME-DOMAIN EMI MEASUREMENT SYSTEM

No.	Description
1	Antenna HL562, Rohde & Schwarz
2	Switching unit RSU, Rohde & Schwarz
3	Amplifier ZFL-1000LN, Mini-Circuits
4	Lowpass-filter SLP-1000, Mini-Circuits
5	Oscilloscope TDS7104, Teletronix
6	PC (IBM compatible)
7	Receiver ESCS30, Rohde & Schwarz

III. SIGNAL PROCESSING

A. Data acquisition

The data acquisition process for the time domain measurement is shown in Fig. 3. After the data acquisition with the oscilloscope, the signal is transformed from time-domain to frequency-domain. The errors due to the frequency characteristics of antenna, transmission line, amplifier and anti-aliasing filter are corrected by signal processing.

B. Error Correction of the measurement system

In order to obtain an accurate spectrum from the time-domain measurements the frequency characteristics of the time-domain measurement system has to be compensated.

0-7803-7239-5/02/$10.00 © 2002 IEEE

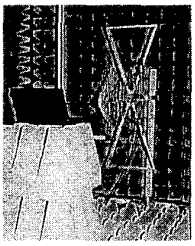

Fig. 2. Measurement scenario (distance between laptop and antenna is 1 m)

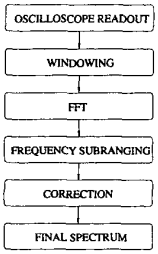

Fig. 3. Process of data acquisition

In Fig. 4 the antenna factor $H_{AF}(f)$ and the amplifier gain $H_{Amp}(f)$ are shown. The antenna factor depends on the effective antenna length, the antenna impedance and the input impedance of the amplifier. In Fig. 5 the measured filter frequency response $H_{LP}(f)$, and the cable losses $H_{Cable}(f)$ are shown. So the calculated spectrum from the time-domain data is corrected considering the total transfer function $H_{CF}(f)$ as follows:

$$H_{CF}(f) = H_{AF}(f)H_{Amp}(f)H_{LP}(f)H_{Cable}(f) \quad (1)$$

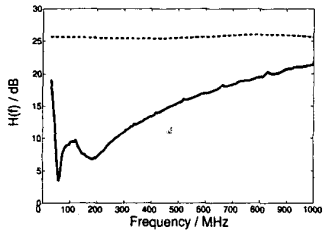

Fig. 4. — Antenna Factor $H_{AF}(f)$ in dB(1/m), – – – Amplifier Gain $H_{Amp}(f)$ in dB

C. Comparison with EMI receiver

For comparison of the time-domain measurements with the EMI receiver measurements the filter characteristic and

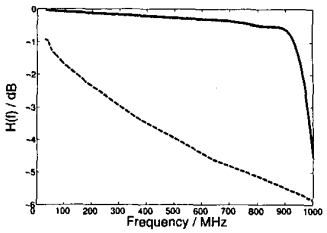

Fig. 5. — Filter Frequency Response $H_{LP}(f)$, – – – Cable losses $H_{Cable}(f)$

the detector type of the EMI receiver have to be taken into account. The measured IF filter characteristics of the EMI receiver have to be taken in account in the spectrum calculation via FFT or Periodogram. For using peak-, average- or quasi-peak detectors a time domain modelling of the detector circuit have to be implemented in the valuation of the calculated frequency spectrum.

IV. Comparison: Time-Domain Measurement System with EMI Receiver

In this section results from the time-domain measurement system with the application of several signal processing algorithm is compared with the results of a conventional EMI receiver.

A. Model of the EMI receiver

To develops an equivalent system behavior for the time-domain EMI measurement system, an accurate system model for the EMI receiver is necessary. The block diagram of a conventional EMI receiver is shown in Fig. 6. Table II summarizes the components of the EMI receiver.

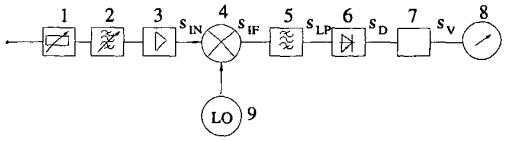

Fig. 6. EMI receiver block diagram

The following equations show the signal stream from the input to the display unit of the EMI receiver. The mixer output signal in the frequency-domain is given by:

$$S_{IF}(f) = S_{IN}(f - f_{LO}) \quad (2)$$

This yields the following output signal of the IF filter:

$$S_{LP}(f) = H_{LP}(f)S_{IF}(f) \quad (3)$$

The detector output signal in the time-domain is given by:

TABLE II
EMI RECEIVER

No.	Description
1	Voltage divider
2	RF selection filter
3	Amplifier
4	Mixer
5	IF filter
6	Detector
7	Valuation unit
8	Display unit
9	Local oscillator

$$s_D(t) = \frac{1}{\Delta t}\int_{(n-1)\Delta t}^{n\Delta t} |s_{LP}(t)|dt \quad (4)$$

The use of different detector types yields to a case differentiation. The valuation unit output signal for a peak measurement in the time-domain is given by:

$$s_V(t) = MAX\{s_D(t)|n \in \{1...N\}\} \quad (5)$$

The valuation unit output signal for a average measurement in the time-domain is given by:

$$s_V(t) = \frac{1}{N\Delta t}\int_0^{N\Delta t} s_D(t)dt \quad (6)$$

B. Signal processing with Fast-Fourier Transform (FFT)

A comparison between the classical Fast-fourier Transform (FFT), Bartlett and Welch Periodogram and the measured results of an commercial EMI receiver using the peak- and average-detector (100 ms/step dwell time) shows an average deviation in the amplitude spectrum below 3 dB for a frequency range of 30 up to 1000 MHz. In Fig. 7 the comparison between the FFT and the EMI receiver in peak-detector mode is shown.

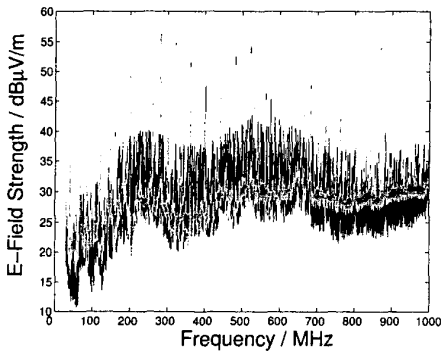

Fig. 7. Comparison: FFT (black line) and EMI receiver (gray line)

C. Signal processing with Periodogram

The EMI spectrum is computed from the time-domain signal using the Bartlett and Welch Periodogram. Both methods are based on the averaging of the spectra obtained by FFT from segments of the time signal. In the Bartlett method which is a special Periodogram method, the time domain sequence x(m) is divided into P nonoverlapping segments, where each segment has length D. For each segment, the Periodogram is computed and the Bartlett power spectral estimate is obtained by averaging the Periodograms for the P segments. The frequency spectrum calculated by the Bartlett Periodogram [5] is given by:

$$P_B^{(p)}(f) = \frac{1}{P}\sum_{p=0}^{P-1}\frac{1}{DT}\left|T\sum_{m=0}^{D-1} x^{(p)}[m]e^{-j2\pi fmT}\right|^2 \quad (7)$$

By this averaging of the spectrum the variance of the spectrum estimation is reduced by a factor P, however at the expense of a reduction of the frequency resolution by a factor P [6]. Welch [7] has modified Bartletts method by using windowed data segments overlapping in time. The overlapping is used for further reducing the Periodogram variance while the windowing is applied to reduce the spectral leakage associated with finite observation intervals. The frequency spectrum calculated by the Welch Periodogram [5] is given by:

$$P_W^{(p)}(f) = \frac{1}{P}\sum_{p=0}^{P-1}\frac{1}{UDT}\left|T\sum_{m=0}^{D-1} x^{(p)}[m]e^{-j2\pi fmT}\right|^2 \quad (8)$$

U is the discrete-time window energy of the used window function $w[m]$ as defined as follows:

$$U = T\sum_{m=0}^{D-1} w^2[m] \quad (9)$$

Fig. 8 and Fig. 9 show the comparison between the Bartlett Periodogram and the EMI receiver in average-detector mode, and the Welch Periodogram and the EMI receiver in average-detector mode, respectively.

V. MEASUREMENT EVALUATION

The average deviation between the spectrum calculated from the time domain data and spectrum from the EMI receiver is below 3 dB over a frequency range of 30 up to 1000 MHz. The measurement error depends on the statistical properties of the interferences. One reason for the deviation is the the non-static EMI spectrum of the laptop.

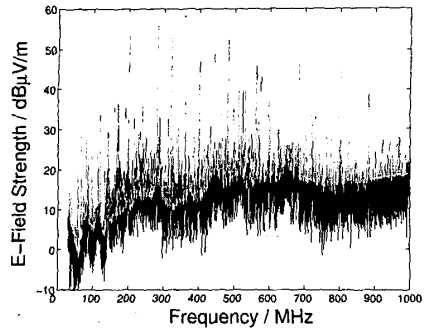

Fig. 8. Comparison: Bartlett Periodogram (black line) and EMI receiver (gray line)

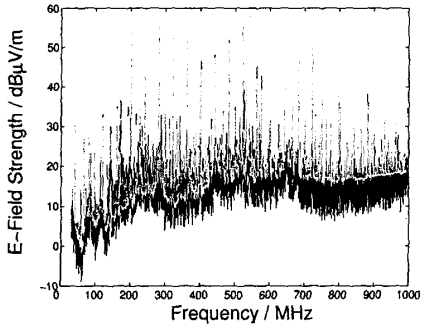

Fig. 9. Comparison: Welch Periodogram (black line) and EMI receiver (gray line)

A. Statistical evaluation

In Fig. 10 the FFT calculated spectrum for 30 independent measurements is shown. At 200 MHz (= clock frequency of the laptop) a steady E-Field amplitude over 30 measurements is detectable. In the frequency range from 400 to 500 MHz a strong variation of the short-time spectrum with time can be observed. In such non-stationary interferences the time domain measurement system is capable to give information about the non-stationary behavior of the EUT, within a short measurement time.

B. Measurement time

The main advantage of an time-domain emission measurement method is the reduced measurement time. Table III a detailed itemization of the required measurement time is shown. According to the standards the EMI receiver work in the peak-detector mode and has a dwell time of 100 ms/step. The measured frequency range is 30 MHz up to 1 GHz.

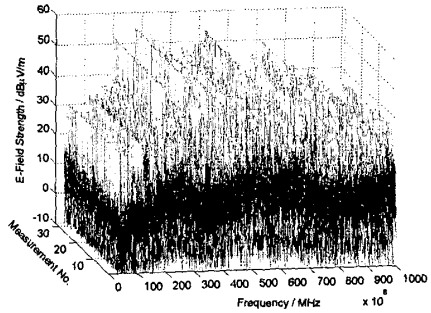

Fig. 10. Comparison between 30 FFT measurements

TABLE III
MEASUREMENT AND PROCESSING TIME

	Oscilloscope	EMI-receiver
data length	64 kSample	19 kSample
measurement time	13μsec.	40 min.
readout time	100 msec.	-
computation time	2 min.	-
total time (approx.)	2.5 min	40 min.

VI. Conclusion

The shown time-domain EMI measurement system allows to reduce the time required for the measurement by a factor of 10 in comparison to a conventional superheterodyne EMI receiver. Three signal processing methods to calculate the spectrum from the data in time-domain has been shown: Fast-fourier Transform, Bartlett and Welch Periodogram. The averaged measurement deviation between the time-domain measurement system and the EMI receiver is below 3 dB over the frequency range of 30 to 1000 MHz.

References

[1] C. Keller, K. Feser, "Fast Emission Measurement In Time Domain", *EMC Zürich*, Zürich, Paper No. 70K7, February 2001.

[2] Christos Christopoulos, "Principles and Techniques of Elektromagnetic Compatibility", *CRC Press*, ISBN 0-8493-7892-3, 1995.

[3] Edwin L. Bronaugh, "An Advanced Electromagnetic Interference Meter for the Twenty-First Century" *EMC Zürich*, Zürich, Paper No 42 H5, pp. 215-219, March 1989.

[4] Edwin L. Bronaugh, John D. M. Osburn, "New Ideas in EMC Instrumentation and Measurement" *EMC Zürich*, Zürich, Paper No. 58J1, pp. 323-326, 1993.

[5] S.L. Marple Jr., "Digital Spectral Analysis with Applications", *Prentice-Hall*, Inc., ISBN 0-8493-7892-3, 1987.

[6] H. C. So, Y. T. Chan, Q. Ma, P. C. Ching, "Comparison of Various Periodograms for Sinusoid Detection and Frequency Estimation", *IEEE Transactions on Aerospace and Elektronic Systems*, Vol. 35, No. 3, pp. 945-952, July 1999.

[7] Peter D. Welch, "The Use of Fast Fourier Transform for the Estimation of Power Spectra: A Method Based on Time Averaging Over Short, Modified Periodograms", *IEEE Transactions on Audio and Electroacoustics*, Vol. AU-15, No.2, pp. 70-73, June 1967.